Title
Quantification of vessel-specific coronary perfusion territories using minimum-cost path assignment and computed tomography angiography: Validation in a swine model

Journal
Journal of Cardiovascular Computed Tomography, 12(5)

ISSN
1934-5925

Authors
Malkasian, Shant
Hubbard, Logan
Dertli, Brian
et al.

Publication Date
2018-09-01

DOI
10.1016/j.jcct.2018.06.006

Peer reviewed

HHS Public Access

Author manuscript

J Cardiovasc Comput Tomogr. Author manuscript; available in PMC 2019 September 01.

Published in final edited form as:

J Cardiovasc Comput Tomogr. 2018 ; 12(5): 425–435. doi:10.1016/j.jcct.2018.06.006.

Quantification of vessel-specific coronary perfusion territories using minimum-cost path assignment and computed tomography angiography: Validation in a swine model

Shant Malkasian, **Logan Hubbard**, **Brian Dertli**, **Jungnam Kwon**, **Sabee Molloi***

Department of Radiological Sciences, University of California Irvine, Irvine, CA, 92697, USA

Abstract

Background—As combined morphological and physiological assessment of coronary artery disease (CAD) is necessary to reliably resolve CAD severity, the objective of this study was to validate an automated minimum-cost path assignment (MCP) technique which enables accurate, vessel-specific assignment of the left (LCA) and right (RCA) coronary perfusion territories using computed tomography (CT) angiography data for both left and right ventricles.

Methods—Six swine were used to validate the MCP technique. In each swine, a dynamic acquisition comprised of twenty consecutive volume scans was acquired with a 320-slice CT scanner following peripheral injection of contrast material. From this acquisition the MCP technique was used to automatically assign LCA and RCA perfusion territories for the left and right ventricles, independently. Each animal underwent another dynamic CT acquisition following direct injection of contrast material into the LCA or RCA. Using this acquisition, reference standard LCA and RCA perfusion territories were isolated from the myocardial blush. The accuracy of the MCP technique was evaluated by quantitatively comparing the MCP-derived LCA and RCA perfusion territories to these reference standard territories.

Results—All MCP perfusion territory masses ($Mass_{MCP}$) and all reference standard perfusion territory masses ($Mass_{RS}$) in the left ventricle were related by $Mass_{MCP} = 0.99Mass_{RS}+0.35$ g ($r = 1.00$). $Mass_{MCP}$ and $Mass_{RS}$ in the right ventricle were related by $Mass_{MCP} = 0.94Mass_{RS}+0.39$ g ($r = 0.96$).

Conclusion—The MCP technique was validated in a swine animal model and has the potential to be used for accurate, vessel-specific assignment of LCA and RCA perfusion territories in both the left and right ventricular myocardium using CT angiography data.

Keywords

Cardiovascular disease; Angiography; Computerized tomography; Imaging; Coronary artery disease; Myocardium

*Corresponding author. Department of Radiological Sciences, Medical Sciences I, B-140, University of California, Irvine, CA, 92697, USA., symolloi@uci.edu (S. Molloi).

Appendix A. Supplementary data

Supplementary data related to this article can be found at http://dx.doi.org/10.1016/j.jcct.2018.06.006.

1. Introduction

Coronary artery disease (CAD) and its resultant ventricular dysfunction are strongly predictive of future cardiac events. However, when CAD risk is appropriately stratified and managed, long-term outcomes are significantly improved.[1,2] Appropriate stratification of CAD requires both morphological and physiological data to reliably assess the true severity of disease.[3–7] Such stratification is often accomplished noninvasively with single-photon emission computed tomography (SPECT), cardiac magnetic resonance (CMR), positron-emission tomography (PET), or dynamic computed tomography (CT) perfusion; modalities that provide relevant perfusion data.

To incorporate corresponding morphological information with this perfusion data, the American Heart Association's (AHA) 17-segment model[8] of the heart is commonly used in the absence of angiographic data. In the 17-segment model, the left ventricle is segmented into seventeen virtual perfusion territories that are assigned to the left anterior descending (LAD), left circumflex (LCx), or right coronary artery (RCA), respectively. Nevertheless, despite the 17-segment model's clinical merit, it is unable to account for coronary morphological variation; thus, coronary perfusion territories are commonly mis-assigned by the model, leading to misinterpretation of perfusion defects.[9–13] Additionally, the 17-segment model does not provide any assessment of the right ventricular myocardium, yet CAD in the RCA is highly prevalent.[14] Given these limitations, there exists a clinical need for improved vessel-specific morphological and physiological assessment of CAD in both ventricles.[11]

With the advent of CT and MR angiography, in addition to hybrid PET/CT and SPECT/CT imaging methods, morphological data is becoming increasingly accessible. Several studies have even gone on to illustrate that such morphological data can be used to algorithmically assign vessel-specific perfusion territories.[15–21] Nonetheless, most of these reports lack robust quantitative validation of their myocardial assignment algorithm's accuracy versus a true reference standard. Additionally, many of these studies have only validated coronary perfusion territory assignment on the epicardial surface of the left ventricle.

Hence, the purpose of this study was to thoroughly validate a minimum-cost path assignment (MCP) technique that enables accurate, vessel-specific assignment of the left and right coronary arterial perfusion territories throughout the full thickness of the left and right ventricular myocardium using computed tomography (CT) angiography data.

2. Methods

2.1. General methods

The study was approved by the Animal Care Committee and Institutional Review Board for the Care of Animal Subjects and was performed in agreement with the "Position of the American Heart Association on Research Animal Use." All data was prospectively acquired between 12/2014 and 07/2016. Specifically, the MCP technique was validated in six male Yorkshire swine (42 ± 9 kg). All swine underwent dynamic CT imaging, once following peripheral intravenous contrast injection and at least once following intracoronary contrast

injection in the left or right main coronary arteries (LCA and RCA). A total of six peripheral intravenous contrast injection acquisitions were acquired, while a total of fifteen reference standard intracoronary injection datasets were acquired. The peripheral contrast injection acquisitions were used for MCP perfusion territory quantification, while the intracoronary injection data was used for extraction of "blushed" and "non-blushed" reference standard perfusion territories. The LCA and RCA perfusion territories obtained with the MCP technique (LCA_{MCP} and RCA_{MCP}) were quantitatively compared to the "blushed" and "non-blushed" reference standard LCA and RCA perfusion territories (LCA_{RS} and RCA_{RS}) obtained from intracoronary LCA and RCA contrast injections through mass and spatial correspondence analysis. Overall, MCP territories were independently derived and validated for the left and ventricular right ventricular myocardium. Additionally, MCP territories were independently derived and validated for the whole heart myocardium, which, in turn, included both the left and right ventricular myocardium.

2.2. Animal protocol

Anesthesia was induced via intramuscular injection of Telazol (4.4 mg/kg), Ketamine (2.2 mg/kg), and Xylazine (2.2 mg/kg), and was maintained after intubation (Covedien, Mansfield, MA) through ventilation (Highland Medical Equipment, Temecula, CA) with an oxygenair-mixture containing 1.5–2.5% Isoflurane (Baxter, Deerfield, IL). Electrocardiogram, O_2 saturation, temperature, blood pressure, and end-tidal CO_2 were monitored and a warming blanket (HTP-1500, Adroit Medical Systems, Loudon, TN) was used to prevent hypothermia.

Using the modified Seldinger technique[22] under ultrasound guidance (Vivid E9, GE Healthcare, IL), catheter sheaths (AVANTI®, Cordis Corporation, Miami Lakes, FL) were placed in both femoral veins and in the right carotid artery. The right femoral vein was used for drug and fluid administration. The left femoral vein was used for peripheral contrast injection. The carotid sheath was used for invasive blood pressure monitoring as well as coronary catheter introduction. Specifically, under fluoroscopic guidance, a Judkins right guide catheter (Cordis Corporation, Miami Lakes, FL) was used to engage the left and right coronary ostia. The guide catheter was then used for intracoronary injection of contrast into the LCA or RCA during dynamic CT imaging, resulting in myocardial "blush" in each perfusion territory, respectively. During CT imaging, animals underwent an expiratory breath hold for the duration of the image acquisition.

2.3. Computed tomography (CT) imaging protocol

To derive MCP perfusion territories (LCA_{MCP} and RCA_{MCP}), dynamic CT data was acquired following peripheral contrast (Isovue 370 mg/mL, 1 mL/kg, 5 mL/s) and saline (0.5 mL/kg, 5 mL/s) injection via the femoral vein. For the determination of reference standard perfusion territories (LCA_{RS} and RCA_{RS}), dynamic CT data was acquired following intracoronary contrast (Isovue 50 mg/mL, 15 mL, 2 mL/s) injection via the guide catheter into the LCA or RCA. For both injection schemes, twenty consecutive volume scans were prospectively acquired with a multi-detector CT scanner (Aquilion One, Toshiba American Medical Systems, Tustin, CA) at 100 kVp and 200 mA, using 320 × 0.5 mm detector collimation with a gantry rotation speed of 0.35 s. Images were acquired using prospective

ECG-gating. Each acquisition, consisting of twenty volume scan, yielded an estimated effective dose of 26.4 mSv, based on a previous study using the same imaging system and imaging parameters.[23] Full projection data was used to avoid partial scan artifacts and all volume scans were reconstructed at 75% of the R-R interval using an FC03 kernel with standard beam hardening corrections. Image datasets from the same animal were reconstructed with the same voxel size. All images were reconstructed with an in-plane resolution of 512 × 512 pixels. Depending on the field-of-view, the reconstruction voxel size ranged from 0.43 × 0.43 × 0.50 mm to 0.79 × 0.79 × 0.50 mm. To allow for adequate renal clearance of contrast, each intracoronary contrast injection acquisition was performed at least 10 min after each peripheral intravenous contrast injection acquisition. Subsequent intracoronary contrast injection acquisitions were also acquired at least 10 min apart.

2.4. Minimum-cost path (MCP) image processing

Based on previous post-mortem swine analysis, it is known that myocardial tissue is perfused by its nearest coronary artery.[18,24] Hence, the MCP technique was designed to model these prior findings by determining the minimum distance, bounded within the heart, between each voxel of the myocardium and each coronary artery. To validate the MCP technique, the peripheral intravenous contrast injection scans and intracoronary injection volume scans from the same animal were first registered, using an affine deformable registration algorithm,[25] to a single maximally enhanced intravenous injection volume. The registered intravenous injection volume scans were then combined into a single maximum intensity projection (MIP) volume, from which the left ventricle, right ventricle and whole heart (both left and right ventricle) myocardium were semi-automatically segmented using a Vitrea workstation (Vitrea fX version 6.0, Vital Images, Inc., Minnetonka, MN). Semi-automatic extraction of the LAD, LCx and RCA centerlines was also performed using the same Vitrea workstation (Fig. 1).

Using a myocardial mask and centerlines of the LAD, LCx, and RCA, MCP was then performed separately on the left ventricle, right ventricle and whole heart, using the Insight Segmentation and Registration Toolkit.[26] Specifically, the vessel centerlines were used as seed points to create three separate distance maps through the myocardium using a Fast-Marching algorithm.[27] Using these distance maps, the minimum–cost path from each voxel of myocardium to each coronary centerline was used to assign each voxel to its closest supplying artery. This resulted in a vessel-specific perfusion territory for each coronary artery (LAD_{MCP}, LCx_{MCP} and RCA_{MCP}). This same process was performed three separate times, using the left ventricle, right ventricle, and whole heart masks, independently. This yielded coronary-specific assignment of the LAD_{MCP}, LCx_{MCP} and RCA_{MCP}, for each segmentation. The MCP technique, performed using the whole heart segmentation, is detailed in Fig. 2.

2.5. Reference standard (RS) image processing

The registered reference standard intracoronary injection volume scans were also combined into separate LCA injection and RCA injection MIP volumes, from which the “blushed” and “non-blushed” LCA and RCA perfusion territories were automatically segmented. As no ventricular blood pool opacification was present in intracoronary contrast injection

acquisition MIPs, the whole heart myocardial mask from the former semi-automatic segmentation was first used to segment the entire myocardium from these MIPs. A median filter was applied to each MIP, followed by automated region growing segmentation to extract the “blushed” and “non-blushed” LCA and RCA perfusion territories. For each region growing segmentation, the ostium of the coronary artery which was cannulated and directly injected with contrast was chosen as a seed point, and was iteratively grown into the whole heart myocardium, with the median Hounsfield Unit (HU) between “blushed” and “non-blushed” myocardium used as the cutoff. As such, each intracoronary injection acquisition resulted in two separate reference standard perfusion territories, one from the “blushed” myocardium and one from the “non-blushed” myocardium. A summary of these image processing steps is illustrated in Fig. 3.

After MCP perfusion territories (LAD_{MCP}, LCx_{MCP} and RCA_{MCP}) were determined, and reference standard perfusion territory (LCA_{RS} and RCA_{RS}) extraction was complete, LAD_{MCP} and LCx_{MCP} were combined into a single left coronary artery MCP perfusion territory (LCA_{MCP}). All “blushed” and “nonblushed” reference standard perfusion territories of the same vessel were pooled together. The LCA_{MCP} and RCA_{MCP} perfusion territories were then quantitatively compared to LCA_{RS} and RCA_{RS} perfusion territories. LCA_{RS} and RCA_{RS} were first determined for the whole heart myocardium, after which they were segmented for only the left and right ventricle using the previously described left and right ventricular masks. These whole heart and ventricle-specific segmentations allowed direct and independent comparison of MCP to the corresponding reference standard whole heart, left ventricle, and right ventricle perfusion territories.

2.6. Bull’s eye plot visualization

Two-dimensional bull’s eye plots were also provided for the right and left ventricles to further detail the coronary perfusion territories. This was achieved using a previously reported method.[28] Both the left and right ventricles were sampled into 100 slabs, perpendicular to the long axis of the heart through averaging. Within each slab, 360 equidistant samples were then taken radially from the center of the left ventricle. This was done for both the left and right ventricles, as well as for the rastered coronary centerlines, to yield bull’s eye plots for the entire myocardium.

2.7. Myocardium at-risk simulation

Myocardium at-risk distal to a stenosis in a single animal was also assessed through simulation. Specifically, after determining LAD_{MCP}, LCx_{MCP} and RCA_{MCP} in the left ventricle, the position of a hypothetical stenosis was designated along the LAD centerline. MCP assignment was then performed in the LAD_{MCP} territory alone using the LAD vessel centerlines proximal and distal to the simulated stenosis, resulting in further delineation of the LAD_{MCP} territory into proximal and distal components. In total, three different LAD stenosis locations were evaluated for myocardium at-risk comparison.

2.8. Statistical approach

In order to rigorously evaluate the accuracy of the MCP technique, MCP and reference standard perfusion territories for the same coronary artery were directly compared, using

both mass and spatial correspondence. To evaluate mass correspondence, the myocardial mass of the MCP territories were compared to the myocardial mass of reference standard territories via linear regression, root-mean-square error (RMSE), adjusted R^2 (Adj. R^2), concordance correlation coefficient (CCC),[29] Pearson's r (r), and Bland-Altman analysis. 95% Confidence intervals for RMSE, Adj. R,[2] CCC, and r are provided, as [CI_{lower}, CI_{upper}]. Myocardial mass was estimated by multiplying the volume of each MCP or RS territory by the average density of myocardium tissue (1.053 g/mL).[30] To further detail mass correspondence between MCP and reference standard perfusion territories, mass correspondence was performed on each axial slice of one animal. Additionally, the left ventricle mass and mass-percent of LAD_{MCP}, LCx_{MCP} and RCA_{MCP} was measured and compared to a previously reported study.[17] Left ventricle mass-percent of MCP perfusion territories was calculated by dividing the mass of each MCP perfusion territory by the total mass of the corresponding left ventricle. Left ventricle, right ventricle and whole heart myocardial masses were calculated using the segmentation masks derived from the intravenous contrast injection image acquisitions. To evaluate spatial correspondence between MCP and reference standard coronary perfusion territories, Dice's similarity coefficient and mean minimum Euclidean distance were computed. Dice's similarity coefficient is an established method used to quantitatively compare the overlap between separate volume segmentations.[31,32] The mean minimum Euclidean distance, a metric similar to the Hausdorff distance,[33] was used as a metric to assess the distance between MCP and reference standard perfusion territories. To compute the mean minimum Euclidean distance, the surface of MCP and corresponding reference standard territories was determined and converted into sets of 3-dimensional Cartesian points. The shortest distance between each point between the MCP and reference standard perfusion territories was then calculated. Distances were computed through unbounded 3-dimensional space. Finally, these distances were then averaged together, to yield the mean minimum Euclidean distance. When determining mean minimum Euclidean distance, only non-overlapping surface points were used, to remove possible bias caused by utilizing the same myocardial segmentation for both MCP and reference standard perfusion datasets. With the exception of Bland-Altman analysis, reference standard territories of the same coronary artery and acquired from the same animal were averaged together, yielding a total of 12 measurements for each assessment metric (6 LCA_{RS} and 6 RCA_{RS}). Mass and spatial correspondence between MCP and reference standard perfusion territories was performed on the left ventricle, right ventricle and whole heart myocardium, independently. Finally, the tolerance of the MCP technique was calculated using the normalized limits of agreement, determined through Bland-Altman analysis. Specifically, the limit of agreement for the MCP technique in the whole heart myocardium was normalized to the average mass of the whole heart myocardium.

3. Results

3.1. Animal model

A total of six swine (42.0 ± 9.0 kg) were imaged. The average heart rate and mean arterial pressure during imaging were 84 ± 10 beats per minute and 77 ± 9 mmHg, respectively. The average mass of the whole heart for all six animals was 81.44 ± 13.91 g. The average masses

of the left and right ventricles were 68.42 ± 11.60 g and 13.02 ± 2.58 g, respectively. Seven LCA and eight RCA intracoronary injections were made, yielding a total of fifteen reference standard perfusion territory pairs (15 LCA_{RS} and 15 RCA_{RS}). Mass and percent mass correspondence from every intracoronary contrast injection acquisition are detailed in Supplemental Table 1.

3.2. Mass correspondence of left and right ventricle MCP perfusion territories

In the left ventricular myocardium, the average mass of LCA_{MCP} was 55.90 ± 9.98 g and the average mass of LCA_{RS} was 56.00 ± 10.15 g, while the average mass of RCA_{MCP} was 12.52 ± 2.60 g and the average mass of RCA_{RS} was 12.42 ± 3.66 g. Left ventricle MCP mass correspondence is further detailed in Table 1a. For the right ventricular myocardium, the average mass of LCA_{MCP} and LCA_{RS} was 5.11 ± 1.64 g and 5.39 ± 2.03 g, respectively, while the average mass of RCA_{MCP} and RCA_{RS} was 7.90 ± 2.20 g and 7.63 ± 2.35 g, respectively. Right ventricle myocardial mass correspondence is detailed in Table 1b. From linear regression analysis, the left ventricular mass of LCA_{MCP} and LCA_{RS} were related by $Mass_{MCP} = 0.97\ Mass_{RS} + 1.48$ g, while the RCA_{MCP} and RCA_{RS} were related by $Mass_{MCP} = 0.66\ Mass_{RS} + 4.29$ g. Combined, the left ventricular mass of all MCP territories, i.e. both LCA_{MCP} and $RCA_{MCP,}$ were related to the mass of all reference standard territories by $Mass_{MCP} = 0.99\ Mass_{RS} + 0.35$ g. Comprehensive linear regression analysis is provided in Table 2a and Fig. 3a. Similar analysis for right ventricle myocardial perfusion territories are described in Table 2b and Fig. 3b.

3.3. Mass correspondence of whole heart MCP perfusion territories

Additionally, mass correspondence analysis was performed on MCP territories derived for the whole heart by combining both the left and right ventricular masks. For the whole heart myocardium, the average masses of LCA_{MCP} and LCA_{RS} were 61.02 ± 10.21 g and 61.39 ± 10.70 g, respectively, while the average masses of RCA_{MCP} and RCA_{RS} were 20.60 ± 4.42 g and 20.18 ± 5.69 g, respectively. Mass correspondence in the whole heart myocardium is further detailed in Table 1c. For the whole heart myocardium, the mass of all MCP territories were related to all reference standard territories by $Mass_{MCP} = 0.97\ Mass_{RS} + 1.19$ g. Linear regression analysis for the whole heart myocardium is shown in Table 2c and Fig. 3c. Whole heart mass correspondence in one animal was also assessed on a per-axial slice basis, as detailed in Fig. 4. The normalized limit of agreement of the MCP technique in the whole heart was 4.96%.

3.4. Spatial correspondence of left and right ventricle MCP perfusion territories

The mean minimum Euclidean distance between the left ventricle myocardium LCA_{MCP} and LCA_{RS} was 2.56 ± 0.30 mm, while the mean minimum Euclidean distance between the left ventricle myocardium RCA_{MCP} and RCA_{RS} was 3.60 ± 1.08 mm. Overlap of left ventricle myocardium LCA_{MCP} with LCA_{RS} yielded a mean Dice's similarity coefficient of 0.97 ± 0.01. Overlap of left ventricle myocardium RCA_{MCP} with RCA_{RS} yielded a mean Dice's similarity coefficient of 0.86 ± 0.06. Spatial correspondence of the left ventricle myocardial perfusion territories is further described in Table 3a. The mean minimum Euclidean distance between right ventricle myocardium LCA_{MCP} and LCA_{RS} was 9.01 ± 2.78 mm, while the mean minimum Euclidean distance between the right ventricle myocardium RCA_{MCP} and

RCA_{RS} was 7.05 ± 3.02 mm. Overlap of right ventricle myocardium LCA_{MCP} with LCA_{RS} yielded a mean Dice's similarity coefficient of 0.86 ± 0.04. Overlap of right ventricle myocardium RCA_{MCP} with RCA_{RS} yielded a mean Dice's similarity coefficient of 0.87 ± 0.05. Spatial correspondence of the right ventricle myocardial perfusion territories is further described in Table 3b.

3.5. Spatial correspondence of whole heart MCP perfusion territories

Spatial correspondence of MCP to reference standard perfusion territories was performed on MCP territories derived for the whole heart by combining both left and right ventricular masks. The mean minimum Euclidean distance between the whole heart myocardium LCA_{MCP} and LCA_{RS} was 4.10 ± 0.86 mm, while the mean minimum Euclidean distance between the whole heart myocardium RCA_{MCP} and RCA_{RS} was 4.65 ± 1.67 mm. Overlap of LCA_{MCP} with LCA_{RS} yielded a mean Dice's similarity coefficient of 0.96 ± 0.01 in the whole heart myocardium. Overlap of RCA_{MCP} with RCA_{RS} yielded a mean Dice's similarity coefficient of 0.87 ± 0.05 in the whole heart myocardium. Whole heart MCP perfusion territory spatial correspondence is detailed in Fig. 3c.

3.6. LAD_{MCP}, LCx_{MCP}, and myocardium at-risk

Beyond validation of LCA_{MCP}, preliminary analysis of LAD_{MCP} and LCx_{MCP} was also performed, and compared with previously reported LAD and LCx left ventricle mass distributions.[17] Myocardial mass and mass-percent distributions of LAD_{MCP}, LCx_{MCP} and RCA_{MCP} are provided in Table 4. Furthermore, MCP was also used to simulate assessment of myocardium at-risk, distal to a simulated stenosis in one animal, as described in Fig. 5. The figure shows that it is possible to determine myocardial mass at risk distal to a stenosis.

4. Discussion

4.1. General discussion

Le et al.[18,21] initially validated a method to quantify coronary perfusion territories. In their study, Le et al. validated a variation of the MCP technique, using *ex vivo* porcine hearts and micro-CT. The validation studies conducted by Le et al. showed excellent correlation between actual myocardial mass and assigned myocardial mass territories, derived using micro-CT datasets. The MCP technique sought to further explore and improve the method proposed by Le et al. *in vivo.* This study improved upon Le et al.'s method by constraining the MCP technique to distance calculations between myocardial voxels and coronary arteries within the myocardial tissue volume, rather than through unbound space. In the current study, both LCA_{MCP} and RCA_{MCP} showed excellent correspondence to LCA_{RS} and RCA_{RS}, respectively, throughout the whole heart, including the right ventricle. However, as the swine in this study exhibited an average heart rate of 80 beats per minute, motion artifacts were common, causing incomplete segmentation of the right ventricle and RCA, especially with respect to the septal branch of the posterior descending coronary artery. Hence, higher discordance was seen between RCA_{MCP} and $RCA_{RS,}$ likely due to suboptimal assignment of the posterior septum. Additionally, the mean minimum Euclidean distance between right ventricle MCP and reference standard perfusion territories was much higher than that of the left ventricle, due to suboptimal right ventricle reference standard territory segmentation.

Overall, however, MCP showed excellent agreement with reference standard perfusion territories.

4.2. Comparison to previously reported methods

Previous studies have proposed several techniques to improve the assessment of coronary perfusion territories.[15–21] Currently, the AHA 17-segment model[8] is widely used, but several reports demonstrate its limitations.[9–13] An improved model-based approach to determining coronary perfusion territories has been proposed,[19] but is still limited by a predefined model.

Other methods to determine vessel-specific coronary perfusion territories,[16,17,20] based on Seiler et al.,[24] have also been proposed, where each voxel of the left ventricular myocardium is assumed to be perfused by its nearest coronary artery. Faber et al.[20] applied Seiler's method using CT angiography and SPECT for validation ($Mass_{Faber} = 0.92Mass_{SPECT} + 10.32$ g, $R^2 = 0.59$). Kurata et al.[16] conducted a study to assess the accuracy of CTA-derived myocardium at-risk using the Voronoi algorithm and SPECT for validation (r = 0.81 [0.74, 0.87] and mass error = 10%). Ide et al.[17] also conducted a histological validation of CTA-derived perfusion territories for the LAD, LCx and RCA using the Voronoi algorithm and *ex vivo* porcine hearts (r = 0.92 for LAD; r = 0.96 for LCx; r = 0.96 for RCA). Additionally, methods to determine coronary perfusion territories using coronary magnetic resonance have also been proposed,[15] but require invasive cannulation of each coronary artery. However, in nearly all previously reported methods, quantification of coronary perfusion territories was only performed on the left ventricle and only mass correspondence analysis was provided.

In comparison to these prior studies, the MCP technique performs equivalently with respect to mass correspondence analysis. Furthermore, the MCP technique was also assessed for spatial correspondence. These spatial correspondence metrics, such as Dice's similarity coefficient and mean minimum Euclidean distance, show that the MCP technique can accurately determine the spatial distribution of the LCA and RCA perfusion territories in the left ventricle, as well as in the right ventricle and whole heart. Additionally, while direct validation of LAD_{MCP} and LCx_{MCP} was not evaluated in this study, comparisons to mass distributions of LAD, LCx and RCA perfusion territories in the left ventricle, as previously reported by Ide et al.,[17] show that MCP has the potential to provide accurate assessment of the LAD and LCx perfusion territories. Finally, preliminary evaluation of myocardium atrisk distal to a stenosis using MCP illustrates that a clinically significant myocardial defect could be discerned.

4.3. Study limitations

There were limitations associated with this study. First, this study utilized a swine model with high heart rates and significant motion artifact in some cases. The thin right ventricle wall is especially susceptible to motion artifact, causing difficulties in blush segmentation and underestimation of right ventricle mass. To amend this, a dedicated study to further validate the MCP technique in the right ventricle could be implemented, with systolic phase reconstructions used instead. By reconstructing systolic phase datasets, the right ventricular myocardium would be thicker, allowing for more consistent segmentation of right ventricle

myocardial blush. Additionally, to better control for motion artifacts and improve image quality, image registration was employed. While image registration allowed for more direct comparison of MCP and corresponding reference standard perfusion territories, this process may have artificially improved correspondence between the two sets of territories. In the previous validation study conducted by Le et al., myocardial assignment accuracy was shown to be dependent on image quality. Specifically, Le et al. evaluated a variation of the MCP technique, using coronary centerlines truncated at various vessel diameters, illustrating that more extensive coronary centerlines resulted in more accurate approximation of coronary perfusion territories.[18] Furthermore, this study used CT imaging to produce both MCP and reference standard perfusion territories. Because the same imaging modality was used to acquire both MCP and reference standard coronary territories, inherent bias could be present across both MCP and reference standard datasets. Yet, Le et al. has adequately provided *ex vivo* validation of a variation of the MCP technique, illustrating excellent accuracy with *ex vivo* myocardial mass.[18]

This study also was performed on a small sample size; further assessment of the MCP technique on a larger population is still necessary. Additionally, this study utilized healthy swine without CAD. Further investigation is necessary to fully understand how significant CAD will affect the performance of the MCP technique. For example, in the case of a complete coronary occlusion where digital extraction of the coronary artery distal to the occlusion is not possible, the MCP technique may be limited. Yet, given recent work illustrating reliable coronary centerline extraction in patients with coronary calcification and stents,[34] it is anticipated that the MCP technique will be able to accurately determine vessel-specific perfusion territories, even in the presence of moderate focal or diffuse CAD, provided accurate coronary artery and myocardial segmentation is achieved. Furthermore, this study assumed a uniform myocardial density, yet in patients with CAD, myocardial density may be heterogeneous. While more investigation is necessary of fully understand how different pathologies affect, as previously mentioned, a variation of the MCP technique was sufficiently validated through comparison with actual myocardial mass.[18,21] Beyond CAD, the MCP technique will be limited in assessing collateralization, as they may be too small to visualize.

In comparison to methods which use the Voronoi algorithm to determine coronary perfusion territories, the MCP technique may be computationally more expensive. Typically, these methods create a mesh surface of the epicardium and endocardium, over which the Voronoi algorithm is applied. This reduces the computational cost of these methods. The MCP technique assigns all voxels of the myocardium to its nearest coronary artery, rather than extrapolating assignment for sub-endocardial voxels, as proposed by groups applying the Voronoi algorithm.[16,17]

It is important to note that in this study, the left ventricle, right ventricle and whole heart MCP perfusion territories were derived using a dynamic CT acquisition, rather than a standard CTA acquisition. However, such an acquisition scheme was used solely to validate MCP in the right ventricle and whole heart, but is not necessary for MCP in the left ventricle. Specifically, MCP in the left ventricle can be derived using only a standard CTA dataset to yield left ventricle, coronary-specific perfusion territories. Hence, the MCP

technique could be integrated with current clinical CTA methods to provide assessment of coronary perfusion territories in the left ventricle. Nevertheless, whole heart and right ventricle assessment using the MCP technique require simultaneous coronary and biventricular opacification. Fortunately, low-dose clinical CTA examinations that acquire biventricular and coronary opacification have already been proposed and implemented using a 64-slice CT system.[35] While a 320-slice CT scanner was utilized, it is expected that coronary perfusion territories could be determined with MCP using more widely available 64-slice and 128-slice CT scanners, provided accurate coronary centerline and myocardial segmentation is possible. Additionally, CT perfusion conveniently acquires biventricular and coronary opacification, as well as myocardial perfusion, in a single low dose examination,[23,36,37] thus MCP could easily be integrated with future imaging protocols. CT was used exclusively in this study, but the MCP technique has the potential to be applied to any imaging modality that provides an image of the myocardium and coronary arteries.

4.4. Conclusion

The MCP technique may provide a means to objectively delimit vessel-specific perfusion territories in the heart. Using mass correspondence, as well as spatial correspondence, such as mean minimum Euclidean distance and Dice's similarity coefficient, the MCP technique has been robustly validated in the left and right ventricular myocardium, as well as in the whole heart, with a normalized limit of agreement of 4.96% in the whole heart. Furthermore, it is anticipated that the MCP technique may have the potential to accurately assign the coronary perfusion territories of the LAD and LCx, as well as quantify the myocardial mass at-risk distal to a stenosis, although further validation is necessary. Thus, given the results, the MCP technique has the potential to improve CAD assessment through accurate and automatic delineation of vessel-specific myocardial perfusion territories using only CT angiography data.

Supplementary Material

Refer to Web version on PubMed Central for supplementary material.

Acknowledgements

The authors would like to thank Mr. Travis Johnson for his technical support in completion of this work.

Sources of funding

This work was supported in part by funds from the Department of Radiological Sciences at the University of California, Irvine.

Disclosures

Sabee Molloi, Ph.D., has previously received grants from Toshiba America Medical Systems and Philips Medical Systems. Shant Malkasian, Logan Hubbard, Brian Dertli, and Jungnam Kwon, M.D. do not have any real or apparent conflicts of interest to disclose.

Abbreviations list

CCC	Lin's concordance correlation coefficient

LCA	Left coronary artery
MCP	Minimum-cost path assignment
MCP_{LCA}	Minimum-cost path assigned LCA myocardial perfusion territory
MCP_{RCA}	Minimum-cost path assigned RCA myocardial perfusion territory
RCA	Right coronary artery
RMSE	Root-mean-square error
RS	Reference standard
RS_{LCA}	Reference standard LCA myocardial perfusion territory
RS_{RCA}	Reference standard RCA myocardial perfusion territory

References

1. Fisher L Coronary-artery surgery study (cass) - a randomized trial of coronary-artery bypass-surgery - survival-data. Circulation. 1983;68(5):939–950. [PubMed: 6137292]
2. Varnauskas E Long-term results of prospective randomized study of coronary-artery bypass-surgery in stable angina-pectoris. Lancet. 1982;2(8309):1173–1180. [PubMed: 6128492]
3. Davies RF, Goldberg AD, Forman S, et al. Asymptomatic Cardiac Ischemia Pilot (ACIP) study two-year follow-up: outcomes of patients randomized to initial strategies of medical therapy versus revascularization. Circulation. 1997;95(8):2037–2043. [PubMed: 9133513]
4. Madsen JK, Grande P, Saunamaki K, et al. Danish multicenter randomized study of invasive versus conservative treatment in patients with inducible ischemia after thrombolysis in acute myocardial infarction (DANAMI). Danish trial in Acute Myocardial Infarction. Circulation. 1997;96(3):748–755.
5. Hachamovitch R, Hayes SW, Friedman JD, Cohen I, Berman DS. Comparison of the short-term survival benefit associated with revascularization compared with medical therapy in patients with no prior coronary artery disease undergoing stress myocardial perfusion single photon emission computed tomography. Circulation. 2003;107(23):2900–2907. [PubMed: 12771008]
6. Shaw LJ, Berman DS, Maron DJ, et al. Optimal medical therapy with or without percutaneous coronary intervention to reduce ischemic burden: results from the Clinical Outcomes Utilizing Revascularization and Aggressive Drug Evaluation (COURAGE) trial nuclear substudy. Circulation. 2008;117(10):1283–1291. [PubMed: 18268144]
7. Topol EJ, Nissen SE. Our preoccupation with coronary luminology. The dissociation between clinical and angiographic findings in ischemic heart disease. Circulation. 1995;92(8):2333–2342. [PubMed: 7554219]
8. Cerqueira MD, Weissman NJ, Dilsizian V, et al. Standardized myocardial segmentation and nomenclature for tomographic imaging of the heart. A statement for healthcare professionals from the cardiac imaging committee of the council on clinical cardiology of the american heart association. Circulation. 2002;105(4):539–542. [PubMed: 11815441]
9. Ortiz-Perez JT, Rodriguez J, Meyers SN, Lee DC, Davidson C, Wu E. Correspondence between the 17-segment model and coronary arterial anatomy using contrast-enhanced cardiac magnetic resonance imaging. JACC Cardiovasc. Imag 2008;1(3):282–293.
10. Pereztol-Valdes O, Candell-Riera J, Santana-Boado C, et al. Correspondence between left ventricular 17 myocardial segments and coronary arteries. Eur Heart J. 2005;26(24):2637–2643. [PubMed: 16183694]
11. Thomassen A, Petersen H, Johansen A, et al. Quantitative myocardial perfusion by O-15-water PET: individualized vs. standardized vascular territories. Eur Heart J Cardiovasc. Imag 2015:970–976.

12. Javadi MS, Lautamaki R, Merrill J, et al. Definition of vascular territories on myocardial perfusion images by integration with true coronary anatomy: a hybrid PET/CT analysis. J Nucl Med. 2010;51(2):198–203. [PubMed: 20080895]
13. Donato P, Coelho P, Santos C, Bernardes A, Caseiro-Alves F. Correspondence between left ventricular 17 myocardial segments and coronary anatomy obtained by multi-detector computed tomography: an ex vivo contribution. Surg Radiol Anat. 2012;34(9):805–810. [PubMed: 22569833]
14. Rafflenbeul W, Urthaler F, Lichtlen P, James TN. Quantitative difference in “critical” stenosis between right and left coronary artery in man. Circulation. 1980;62(6):1188–1196. [PubMed: 7438354]
15. Carlsson M, Saeed M. Intracoronary injection of contrast media maps the territory of the coronary artery: an MRI technique for assessing the effects of locally delivered angiogenic therapies. Acad Radiol. 2008;15(11):1354–1359. [PubMed: 18995187]
16. Kurata A, Kono A, Sakamoto T, et al. Quantification of the myocardial area at risk using coronary CT angiography and Voronoi algorithm-based myocardial segmentation. Eur Radiol. 2015;25(1): 49–57. [PubMed: 25173626]
17. Ide S, Sumitsuji S, Yamaguchi O, Sakata Y. Cardiac computed tomography-derived myocardial mass at risk using the Voronoi-based segmentation algorithm: a histological validation study. J Cardiovasc Comput Tomogr. 2017;11(3):179–182. [PubMed: 28431861]
18. Le H, Wong JT, Molloi S. Estimation of regional myocardial mass at risk based on distal arterial lumen volume and length using 3D micro-CT images. Comput. Med. Imag. Graph. : the official J.Comput. Med. Imag. Soc 2008;32(6):488–501.
19. Cerci RJ, Arbab-Zadeh A, George RT, et al. Aligning coronary anatomy and myocardial perfusion territories: an algorithm for the CORE320 multicenter study. Cardiovasc. Imag 2012;5(5):587–595.
20. Faber TL, Santana CA, Garcia EV, et al. Three-dimensional fusion of coronary arteries with myocardial perfusion distributions: clinical validation. J Nucl Med. 2004;45(5):745–753. [PubMed: 15136621]
21. Le HQ, Wong JT, Molloi S. Allometric scaling in the coronary arterial system. Int J Cardiovasc Imag. 2008;24(7):771–781.
22. Pettit J Technological advances for PICC placement and management. Adv Neonatal Care. 2007;7(3):122–131. [PubMed: 17844776]
23. Hubbard L, Ziemer B, Lipinski J, et al. Functional assessment of coronary artery disease using whole-heart dynamic computed tomographic perfusion. Cardiovasc. Imag 2016;9(12):1–8.
24. Seiler C, Kirkeeide RL, Gould KL. Measurement from arteriograms of regional myocardial bed size distal to any point in the coronary vascular tree for assessing anatomic area at risk. J. Am. Coll. Cardiol 1993;21:783–797. [PubMed: 8436762]
25. Modat M, Ridgway GR, Taylor ZA, et al. Fast free-form deformation using graphics processing units. Comput. Meth. Progr. Biomed 2010;98(3):278–284.
26. McCormick M, Liu X, Jomier J, Marion C, Ibanez LITK. Enabling reproducible research and open science. Front Neuroinf. 2014;8:13.
27. Sethian JA. A fast marching level set method for monotonically advancing fronts. Proc Natl Acad Sci Unit States Am. 1996;93(4):1591–1595.
28. Termeer M, Olivan Bescos J, Breeuwer M, et al. Visualization of myocardial perfusion derived from coronary anatomy. IEEE Trans Vis Comput Graph. 2008;14(6):1595–1602. [PubMed: 18989015]
29. Lin LI. A concordance correlation coefficient to evaluate reproducibility. Biometrics. 1989;45(1): 255–268. [PubMed: 2720055]
30. Vinnakota KC, Bassingthwaighte JB. Myocardial density and composition: a basis for calculating intracellular metabolite concentrations. Am J Physiol Heart Circ Physiol. 2004;286(5):H1742–H1749. [PubMed: 14693681]
31. Dice LR. Measures of the amount of ecologic association between species. Ecol. 1945;26(3):297–302.

32. Zou KH, Warfield SK, Bharatha A, et al. Statistical validation of image segmentation quality based on a spatial overlap index: scientific reports. Acad Radiol. 2004;11(2):178–189. [PubMed: 14974593]

33. Huttenlocher DP, Klanderman GA, Rucklidge WA. Comparing images using the Hausdorff distance. IEEE Trans Pattern Anal Mach Intell. 1993:15.

34. Yang G, Kitslaar P, Frenay M, et al. Automatic centerline extraction of coronary arteries in coronary computed tomographic angiography. Int.J.Cardiovasc. Imag 2012;28(4):921–933.

35. Kerl JM, Ravenel JG, Nguyen SA, et al. Right heart: split-bolus injection of diluted contrast medium for visualization at coronary CT angiography. Radiology. 2008;247(2):356–364. [PubMed: 18372454]

36. Ziemer BP, Hubbard L, Lipinski J, Molloi S. Dynamic CT perfusion measurement in a cardiac phantom. Int.J.Cardiovasc. Imag 2015;31(7):1451–1459.

37. Hubbard L, Lipinski J, Ziemer B, et al. Comprehensive assessment of coronary artery disease by using first-pass analysis dynamic CT perfusion: validation in a swine model. Radiology. 2018;286(1):93–102. [PubMed: 29059038]

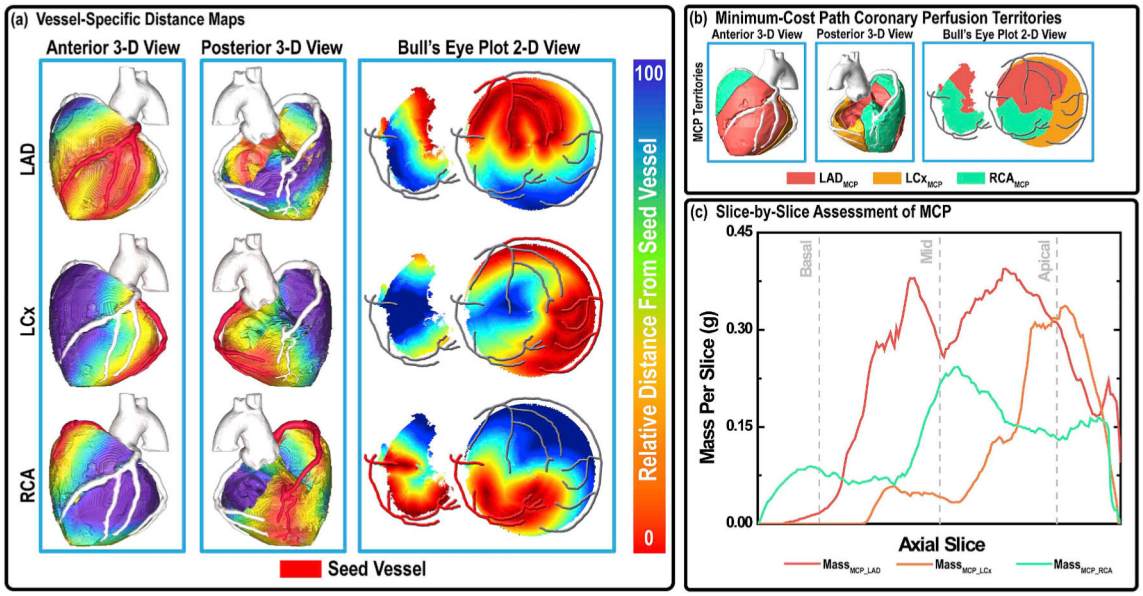

Fig. 1. Minimum-Cost Path assignment method summary.

(a) Distance maps through a whole heart myocardial mask were generated for the LAD, LCx and RCA, using the Fast-Marching algorithm and respective vessel centerline as seed points (red). (b) These distance maps were used to determine the minimum-cost path of each myocardial voxel to each coronary artery, yielding three discrete vessel perfusion territories for each coronary artery in the whole heart. (c) Assessment of mass distribution of LAD_{MCP}, LCx_{MCP} and RCA_{MCP} is also provided, on a per-axial slice basis in the whole heart. This method was applied using only the left ventricle and right ventricle masks, independently, in the same manner, to yield left ventricle and right ventricle MCP territories.

(2-D = Two Dimensional, 3-D = Three Dimensional, LAD = left anterior descending coronary artery, LAD_{MCP} = Minimum-Cost Path assigned LAD myocardial perfusion territory, LCx = left circumflex coronary artery, LCx_{MCP} = Minimum-Cost Path assigned LCx myocardial perfusion territory, RCA = right coronary artery, RCA_{MCP} = Minimum-Cost Path assigned RCA myocardial perfusion territory). (For interpretation of the references to colour in this figure legend, the reader is referred to the Web version of this article.)

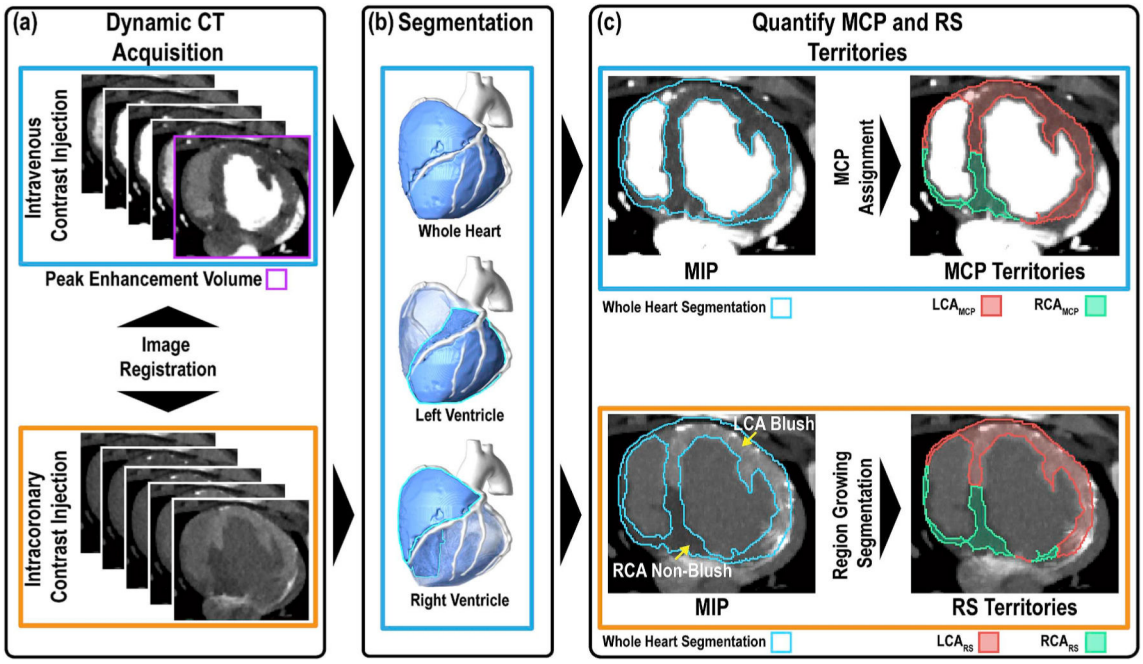

Fig. 2. Image Processing Methods.

(a) First, an intracoronary contrast injection CT acquisition was registered to the peak enhancement volume from the intravenous contrast injection CT acquisition from the same animal. (b) MCP assignment was then performed on the segmented whole heart to yield LCA_{MCP} and RCA_{MCP}, while automated region growing segmentation was performed on the intracoronary contrast injection MIP, using the same whole heart segmentation. Panels outlined in blue depict steps performed on intravenous contrast injection data, while panels outlined in orange depict steps performed on intracoronary contrast injection data. The images shown were acquired from the same animal. While processing in the whole heart is depicted, the same steps were followed, using left and right ventricle masks to derive MCP perfusion territories.

(LCA = left coronary artery, LCA_{MCP} = minimum-cost path assigned LCA myocardial perfusion territory, LCA_{RS} = reference standard LCA myocardial perfusion territory, MCP = minimum-cost path assignment, MIP = maximum intensity projection image, RCA = right coronary artery, RCA_{MCP} = minimum-cost path assigned RCA myocardial perfusion territory, RCA_{RS} = reference standard RCA myocardial perfusion territory). (For interpretation of the references to colour in this figure legend, the reader is referred to the Web version of this article.)

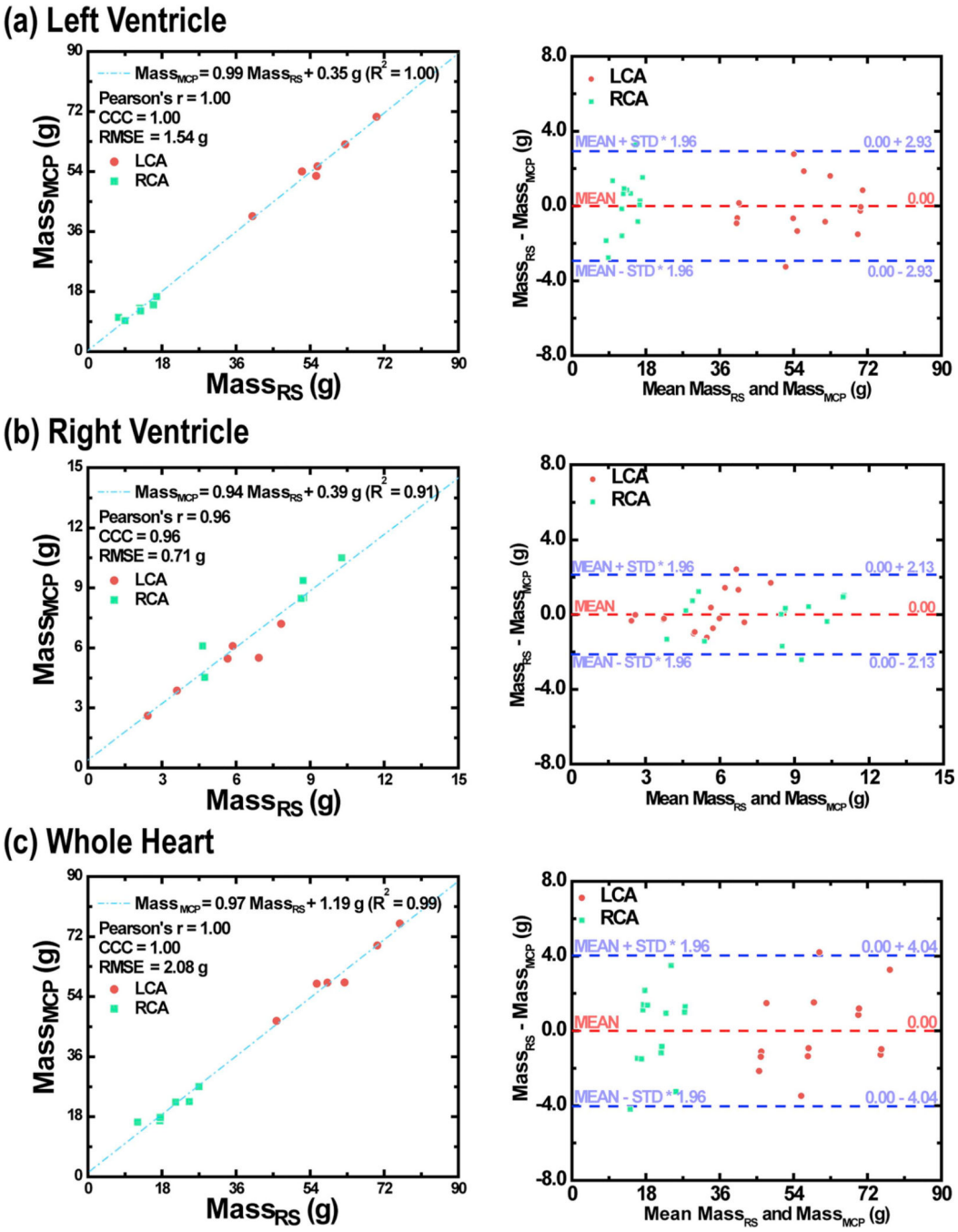

Fig. 3. Linear regression and Bland-Altman analysis of mass correspondence of M_{MCP} and M_{RS} for LCA and RCA territories, in the (a) left ventricle, (b) right ventricle, and (c) whole heart myocardium.

Linear regression analysis displayed above was computed using both LCA and RCA correspondence together. (CCC = concordance correlation coefficient; LCA = left coronary artery; $Mass_{MCP}$ = mass of minimum-cost path-derived coronary territory; $Mass_{RS}$ = mass of reference standard coronary territory; RCA = right coronary artery; RMSE = root-mean-square error).

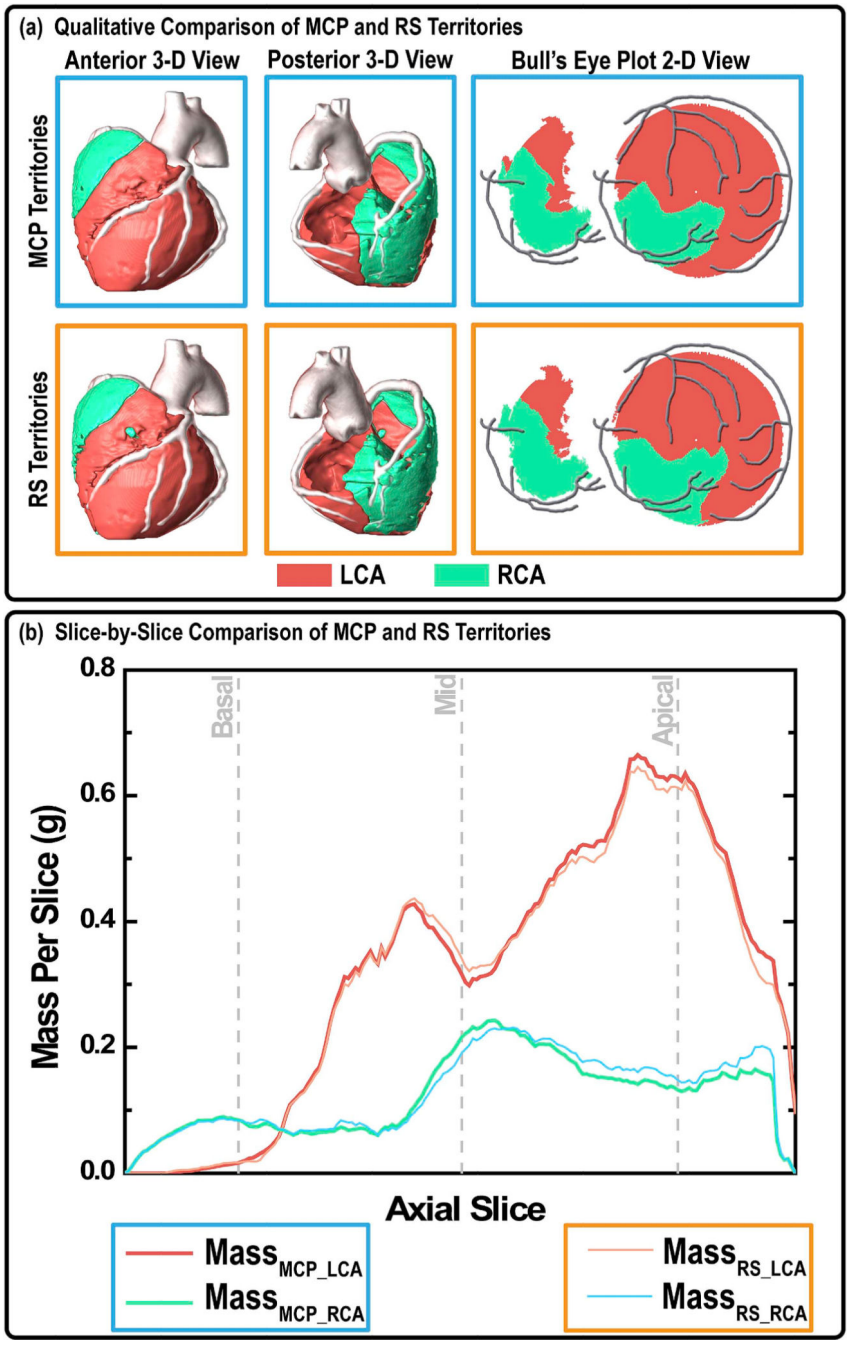

Fig. 4. Whole heart slice-by-slice analysis of mass correspondence of MCP and reference standard myocardial perfusion territories from a single animal.

Slice-by-slice comparison was performed using the Animal 1 dataset. (a) LCA_{MCP} and RCA_{MCP} (blue panels), and LCA_{RS} and RCA_{RS} (orange panels) volumes are shown. Anterior and posterior 3-D volumetric views of MCP and reference standard territories are shown. Right and left ventricle 2-D bull's eye plot projections of MCP and reference standard territories are also shown. The right ventricle 2-D bull's eye plot projection is shown superimposed with the RCA vessel centerline. The left ventricle 2-D bull's eye plot projection is shown superimposed with the LAD, LCx and RCA vessel centerlines.

Quantitative, slice-by-slice analysis is performed by comparing the $Mass_{MCP\_LCA}$ and $Mass_{RS\_LCA}$, as well as $Mass_{MCP\_RCA}$ and $Mass_{RS\_RCA}$.
(2-D = Two Dimensional, 3-D = Three Dimensional, MCP = minimum-cost path assignment, LCA = left coronary artery, $Mass_{MCP\_LCA}$ = minimum-cost path assigned LCA myocardial perfusion territory, $Mass_{RS\_LCA}$ = reference standard LCA myocardial perfusion territory, RCA = right coronary artery, $Mass_{MCP\_RCA}$ = minimum-cost path assigned RCA myocardial perfusion territory, $Mass_{RS\_RCA}$ = reference standard RCA myocardial perfusion territory, RS = reference standard). (For interpretation of the references to colour in this figure legend, the reader is referred to the Web version of this article.)

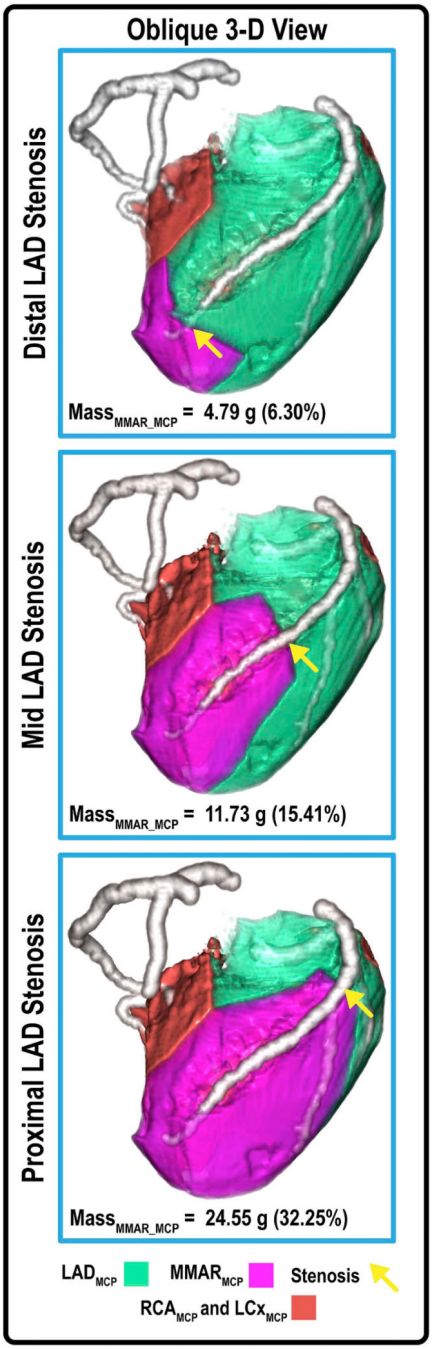

Fig. 5. Evaluation of myocardium at-risk distal of a stenosis in the LAD, using MCP.

An increasingly proximal stenosis was simulated in the LAD. MCP was then used to determine the myocardial mass at-risk distal of the stenosis, in each case. Mass of myocardium at-risk distal of each stenosis is reported as MASS (MASS PERCENT OF TOTAL LEFT VENTRICULAR MYOCARDIUM).

(3-D = Three Dimensional, LAD = left anterior descending coronary artery, LAD_{MCP} = minimum-cost path assigned LAD myocardial perfusion territory, LCx = left circumflex coronary artery, LCx_{MCP} = minimum-cost path assigned LCx myocardial perfusion territory,

$MMAR_{MCP}$ = minimum-cost path assigned myocardial mass at-risk; RCA = right coronary artery, RCA_{MCP} = minimum-cost Path assigned RCA myocardial perfusion territory).

Table 1

Mass correspondence of MCP and reference standard coronary perfusion territories in the (a) left ventricle, (b) right ventricle and (c) whole heart myocardium.

	LCA		RCA	
	$Mass_{MCP}$ (g)	**$Mass_{RS}$ (g)**	**$Mass_{MCP}$ (g)**	**$Mass_{RS}$ (g)**
(a) Left Ventricle				
Animal 1	54.00	52.04 ± 2.22	13.96	15.92 ± 1.83
Animal 2	62.14	62.52 ± 1.73	12.98	12.6 ± 1.73
Animal 3[a]	52.70	55.46	10.24	7.47
Animal 4	40.60	40.02 ± 0.51	12.21	12.79 ± 0.51
Animal 5	70.42	70.17 ± 0.97	16.47	16.72 ± 0.97
Animal 6	55.57	55.82 ± 2.26	9.26	9.00 ± 2.26
MEAN ± STD	55.90 ± 9.98	56.00 ± 10.15	12.52 ± 2.60	12.42 ± 3.66
(b) Right Ventricle				
Animal 1	3.86	3.61 ± 0.03	8.49	8.74 ± 0.04
Animal 2	7.20	7.83 ± 1.50	9.36	8.72 ± 1.50
Animal 3[a]	5.49	6.92	6.09	4.66
Animal 4	6.08	5.87 ± 1.10	4.52	4.74 ± 1.10
Animal 5	5.45	5.66 ± 1.61	10.50	10.29 ± 1.61
Animal 6	2.61	2.43 ± 0.23	8.46	8.64 ± 0.23
MEAN ± STD	5.11 ± 1.64	5.39 ± 2.03	7.90 ± 2.20	7.63 ± 2.35
(c) Whole Heart				
Animal 1	57.86	55.65 ± 2.18	22.46	24.67 ± 1.80
Animal 2	69.34	70.35 ± 0.23	22.34	21.32 ± 0.23
Animal 3[a]	58.19	62.39	16.33	12.13
Animal 4	46.68	45.89 ± 1.57	16.73	17.53 ± 1.58
Animal 5	75.87	75.83 ± 2.20	26.97	27.01 ± 2.20
Animal 6	58.18	58.25 ± 2.03	17.72	17.65 ± 2.04

	LCA		RCA	
	$Mass_{MCP}$ (g)	**$Mass_{RS}$ (g)**	**$Mass_{MCP}$ (g)**	**$Mass_{RS}$ (g)**
MEAN ± STD	61.02 ± 10.21	61.39 ± 10.70	20.60 ± 4.42	20.18 ± 5.69

Data expressed as mass, or mean mass ± standard deviation.

(LCA = left coronary artery, $Mass_{MCP}$ = mass of minimum-cost path coronary territory, $Mass_{RS}$ = mass of reference standard coronary territory, RCA = right coronary artery).

[a]Animal 3 expired after only one intracoronary contrast injection acquisition.

J Cardiovasc Comput Tomogr. Author manuscript; available in PMC 2019 September 01.

Table 2

Linear regression analysis of MCP and reference standard perfusion territories in the (a) left ventricle, (b) right ventricle and (c) whole heart myocardium.

	Linear Regression	RMSE (g)	Adj. R^2	CCC	r
(a) Left Ventricle					
LCA	$Mass_{MCP}$ = 0.97MassRS + 1.48 g	1.71	0.97 [0.75, 1.00]	0.99 [0.89, 1.00]	0.99 [0.89, 1.00]
RCA	$Mass_{MCP}$ = 0.66MassRS + 4.29 g	1.05	0.84 [0.08, 0.98]	0.88 [0.24, 0.99]	0.93 [0.50, 0.99]
LCA + RCA	**$Mass_{MCP}$ = 0.99MassRs + 0.35g**	**1.54**	**0.99 [0.98, 1.00]**	**1.00 [0.99, 1.00]**	**1.00 [0.99, 1.00]**
(b) Right Ventricle					
LCA	$Mass_{MCP}$ = 0.77MassRS + 0.95 g	0.53	0.90 [0.30, 0.99]	0.93 [0.46, 0.99]	0.96 [0.65, 1.00]
RCA	$Mass_{MCP}$ = 0.90MassRS + 1.06 g	0.69	0.90 [0.34, 0.99]	0.95 [0.61, 0.99]	0.96 [0.67, 1.00]
LCA + RCA	**$Mass_{MCP}$ = 0.94MassRs + 0.39g**	**0.71**	**0.91 [0.70, 0.97]**	**0.96 [0.85, 0.99]**	**0.96 [0.85, 0.99]**
(c) Whole Heart					
LCA	$Mass_{MCP}$ = 0.93MassRS + 3.65 g	2.28	0.95 [0.60, 0.99]	0.98 [0.79, 1.00]	0.98 [0.82, 1.00]
RCA	$Mass_{MCP}$ = 0.72MassRS + 5.94 g	1.74	0.83 [0.05, 0.98]	0.90 [0.32, 0.99]	0.93 [0.48, 0.99]
LCA + RCA	**$Mass_{MCP}$ = 0.97MassRs + 1.19g**	**2.08**	**0.99 [0.97, 1.00]**	**1.00 [0.98, 1.00]**	**1.00 [0.99, 1.00]**

Bolded row is plotted in Fig. 3.

For Adj. R^2, CCC and r, 95% confidence intervals (CI) are expressed as [CI_{Lower}, CI_{Upper}].

(Adj. R^2 = Adjusted R^2; CCC = concordance correlation coefficient, LCA = left coronary artery, $Mass_{MCP}$ = mass of minimum-cost path coronary territory, $Mass_{RS}$ = mass of reference standard coronary territory, RCA = right coronary artery, RMSE = root-mean-square error).

Table 3

Spatial correspondence of MCP and reference standard coronary territories in the (a) left ventricle, (b) right ventricle, and (c) whole heart myocardium.

	LCA		RCA	
	MMD (mm)	**DSC**	**MMD (mm)**	**DSC**
(a) Left Ventricle				
Animal 1	2.37 ± 0.01	0.97 ± 0.01	2.56 ± 0.16	0.90 ± 0.01
Animal 2	2.38 ± 0.04	0.96 ± 0.01	5.65 ± 3.69	0.82 ± 0.03
Animal 3[a]	3.03	0.97	3.78	0.79
Animal 4	2.43 ± 0.23	0.97 ± 0.00	3.10 ± 1.05	0.91 ± 0.01
Animal 5	2.28 ± 0.25	0.98 ± 0.00	3.45 ± 1.82	0.91 ± 0.02
Animal 6	2.84 ± 0.33	0.97 ± 0.01	3.06 ± 0.23	0.81 ± 0.06
MEAN ± STD	2.56 ± 0.30	0.97 ± 0.01	3.60 ± 1.08	0.86 ± 0.06
(b) Right Ventricle				
Animal 1	4.44 ± 0.36	0.92 ± 0.01	4.23 ± 1.24	0.96 ± 0.00
Animal 2	12.23 ± 0.90	0.86 ± 0.07	5.62 ± 1.82	0.88 ± 0.08
Animal 3[a]	8.30	0.82	10.08	0.80
Animal 4	11.42 ± 2.72	0.87 ± 0.01	11.42 ± 1.79	0.83 ± 0.05
Animal 5	9.54 ± 2.01	0.87 ± 0.06	4.38 ± 0.91	0.92 ± 0.05
Animal 6	8.14 ± 4.85	0.81 ± 0.11	6.55 ± 3.63	0.94 ± 0.03
MEAN ± STD	9.01 ± 2.78	0.86 ± 0.04	7.05 ± 3.02	0.89 ± 0.07
(c) Whole Heart				
Animal 1	2.54 ± 0.25	0.97 ± 0.01	3.04 ± 0.32	0.92 ± 0.01
Animal 2	4.98 ± 2.38	0.95 ± 0.02	5.90 ± 3.69	0.85 ± 0.05
Animal 3[a]	4.33	0.95	5.36	0.79
Animal 4	4.37 ± 0.50	0.96 ± 0.00	5.92 ± 0.61	0.89 ± 0.02
Animal 5	4.62 ± 1.93	0.97 ± 0.01	3.78 ± 0.78	0.92 ± 0.03
Animal 6	3.75 ± 0.83	0.96 ± 0.01	4.53 ± 1.85	0.88 ± 0.04
MEAN ± STD	4.10 ± 0.86	0.96 ± 0.01	4.65 ± 1.67	0.87 ± 0.05

Data expressed as mean ± standard deviation.

(DSC = Dice's similarity coefficient, LCA = left coronary artery, MMD = mean minimum Euclidean distance, myocardium, RCA = right coronary artery).

[a]Animal 3 expired after only one intracoronary contrast injection acquisition.

Table 4

Absolute and relative coronary perfusion distributions for LAD_{MCP}, LCx_{MCP} and RCA_{MCP} in the left ventricle myocardium.

	LAD	**LCx**	**RCA**
	$Mass_{MCP}$(g)	**$Mass_{MCP}$(g)**	**$Mass_{MCP}$(g)**
Animal 1	36.46 [53.65%]	17.54 [25.81%]	13.96 [20.54%]
Animal 2	38.35 [51.05%]	23.79 [31.67%]	12.98 [17.28%]
Animal 3	31.91 [50.71%]	20.78 [33.03%]	10.24 [16.27%]
Animal 4	28.79 [54.52%]	11.81 [22.36%]	12.21 [23.12%]
Animal 5	43.94 [50.57%]	26.48 [30.47%]	16.47 [18.96%]
Animal 6	32.03 [49.40%]	23.54 [36.32%]	9.26 [14.28%]
MEAN ± STD	35.25 ± 5.47 [51.65 ± 1.99%]	20.66 ± 5.29 [29.94 ± 5.06%]	12.52 ± 2.60 [18.41 ± 3.16%]
Reported by Ide et al.[17]	49.8%	32.2%	25.9%

Data expressed as mass [percent mass], or mass ± standard deviation [percent mass ± standard deviation].

(LAD = left anterior descending coronary artery, LCx = left circumflex coronary artery, M_{MCP} = mass of Minimum-Cost Path-derived coronary territory, RCA = right coronary artery).